Electrochemical Observation of the Photoinduced Formation of Alloyed ZnSe(S) Nanocrystals

Nikolai P. Osipovich,[†] Alexey Shavel,[‡] Sergey K. Poznyak,[†] Nikolai Gaponik,*[,‡] and Alexander Eychmüller[‡]

Physico-Chemical Research Institute, Belarussian State University, 220050 Minsk, Belarus, and Physical Chemistry, Technical University of Dresden, Bergstrasse 66b, 01062 Dresden, Germany

Received: May 21, 2006; In Final Form: July 28, 2006

Electrochemical studies of thiol-capped ZnSe nanocrystals in aqueous solution have demonstrated several distinct oxidation and reduction peaks in the voltammograms, with the peak positions being dependent on the size of the nanocrystals and their photoluminescence quantum efficiency. The evolution of the specific features in the cyclic voltammetric curves of ZnSe NCs as a function of their photochemical treatment is studied. The interpretation of the results based on the approaches previously developed for CdTe NCs is found to be in good correlation with the proposed mechanism of the ZnSe NCs phototreatment, i.e., the formation of a sulfur-enriched surface shell. By this, cyclic voltammetry has been demonstrated to be a powerful method for probing surface states of semiconductor NCs as well as for monitoring the evolution of these states during photochemical processing.

Exposing semiconductor nanocrystals (NCs) post-preparatively to UV−vis radiation allows an increase in their photoluminescence (PL) quantum yields[1−5] as well as the narrowing of their size distributions.[1,6] Depending on specific conditions, photoinduced rearrangements of the surface molecules,[2] photochemical synthesis of an inorganic shell,[3,4] or photoetching of surface defects[1,7,8] were found to be responsible for the improvements observed. For example, irradiation of thiol-capped CdTe NCs in aerated aqueous solution leads to reduction of their size and to an improvement of their quality due to etching of the surface defects.[1] Irradiation of the same type of NCs in deaerated solution in the presence of an excess of cadmium ions and thioglycolic acid (acting as a capping agent) leads to the formation of a passivating CdS shell.[3] The manyfold increase of the PL quantum yields is followed by a blue shift of the optical spectra in the former case and a red shift in the latter.

Recently, a successful synthesis of thiol-capped ZnSe nanocrystals was reported.[4,9] As-prepared nanocrystals possess a weak broad whitish-blue emission that is mainly associated with trap states. However, the irradiation of the thus obtained ZnSe NCs with "white light" leads to a dramatic improvement of the PL properties namely to a narrow UV-blue band-edge emission that reached in the best cases quantum efficiencies of up to 25−30%.[4] This enhancement was explained by the formation of a sulfur enriched shell on the surface of the nanocrystals. Photodestruction of thiol molecules being present in excess in the colloidal solutions is assumed to be the source of the sulfur that together with excess zinc ions is consumed for the shell formation.[4] Figure 1a shows a typical evolution of the absorption and PL spectra of thioglycolic acid (TGA) stabilized ZnSe NCs under the irradiation of a 100 W Xe lamp. The red shift of the first optical transition is a distinguishing feature for increasing NC sizes or the shell formation. The evolution of the PL excitation spectra (Figure 1b) shows a considerable increase of the amount of NCs contributing to the emission at 375 nm. Although the PL maximum is in the near-UV region, the small spectral overlap with the visible region (above 400 nm) appears to be enough to visualize the luminescence of the NC solution after the irradiation (Figure 1b, inset).

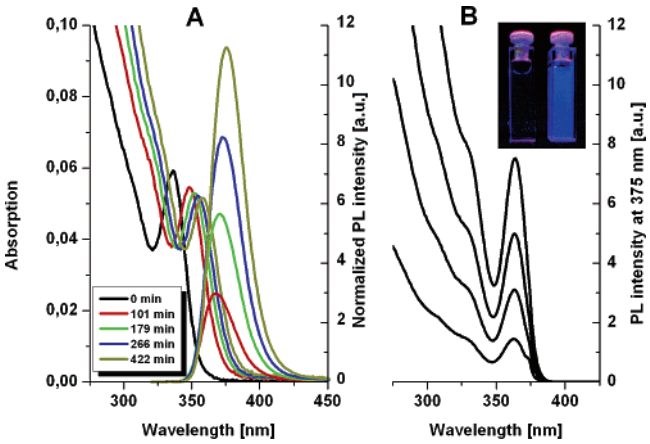

Figure 1. Evolution of the optical properties of ZnSe NCs during illumination (A) and evolution of the PLE spectra ($\lambda_{obs.} = 375$ nm) (B). The inset shows a true color fluorescence image (λ_{ex} 366 nm) of the ZnSe NCs before (left) and after (right) the phototreatment.

Electrochemical methods and, in particular, cyclic voltammetry have successfully been used for the investigation of energy levels in semiconductor NCs.[10−15] Moreover, as has recently been shown that cyclic voltammetry of CdTe[16] and CdSe[15] NCs appears to be sensitive to their surface states. A clear correlation between the properties (band gap and band positions, PL quantum yields, stability) of CdTe NCs and the appearance and shape of specific features in the corresponding cyclic voltammograms was found. The possibility of distinguishing between electrochemical peaks relating to the conduction and valence bands as well as to surface (trap) states was demonstrated.

* Author to whom correspondence should be addressed. E-mail: nikolai.gaponik@chemie.tu-dresden.de.
[†] Belarussian State University.
[‡] Technical University of Dresden.

10.1021/jp063104q CCC: $33.50
Published on Web 09/13/2006

Taking into account the mentioned sensitivity of the electrochemical methods to the NC surface states and the similarity of ZnSe and CdTe NCs with TGA-capping in an aqueous synthesis, the evolution of the surface properties of ZnSe NCs under light irradiation was chosen to be the object for a cyclic voltammetric study presented in this paper.

The ZnSe nanocrystals were synthesized according to the standard procedure.[4,17] During the reflux of the preparation solution the ZnSe nanocrystals grow and fractions with sizes of about 1.5−2 nm are obtained. The size-selective precipitation was applied to the "as prepared" solution of the ZnSe NCs to improve the size distribution and separate the NCs from the byproducts of the synthesis.[1,18] The procedure is based on the NCs precipitation from the crude solution by portion-wise addition of a nonsolvent (2-propanol) and subsequent centrifugation. The precipitate was separated from the supernatant and redissolved in pure water until the concentration was close to that of the initial crude solution. The supernatant underwent the next cycle of the precipitation/dissolution sequence. The resulting fractions with narrower size distributions and well pronounced first optical transitions were chosen for the following experiments.

The photochemical treatment was performed as follows. A 83 μL sample of a size-selected fraction of nanocrystals was added to 10 mL of a fresh solution of $Zn(ClO_4)_2 \cdot 6H_2O$ (16 mM) and TGA (40 mM) at pH 6.6. To assign the anodic peaks and understand better the details of the shell formation the behavior of the ZnSe NCs in a solution of TGA only (40 mM, pH 6.6) and in pure water has been studied as well. The solution was illuminated by the light of a high-pressure Hg lamp equipped with an aqueous IR filter and a filter to cut the UV irradiation with $\lambda < 300$ nm. The total intensity of the photochemically active light in the wavelength range from 300 to 400 nm was about 75 mW cm^{-2}. All these experiments were performed in a quartz cell under open air conditions and under intensive stirring. Aliquots of the solution were taken for spectroscopic and electrochemical measurements after different periods of time. These aliquots were then precipitated by 2-propanol and centrifuged. The precipitates were separated from the supernatant and redissolved in acetate buffer giving stable colloidal solutions. After that the gold electrode (see below) was dipped for 5 min into the buffer solution containing the ZnSe NCs. Our previous study on CdTe NCs showed that the thiol-capped NCs were efficiently absorbed (at least 50% surface coverage) on the gold surface under the conditions used.[16] The electrode with adsorbed ZnSe NCs was thoroughly washed with a fresh buffer solution and replaced into the electrochemical cell as a working electrode for the investigations.

Electrochemical measurements were performed in a standard three-electrode two-compartment cell with a platinum counter electrode and an Ag|AgCl|KCl(sat.) electrode as the reference electrode (+0.201 V vs SHE). All potentials were determined with respect to this reference electrode and were controlled by a conventional potentiostat with a controller. The working electrode compartment of the electrochemical cell was separated from the counter electrode compartment by a fine porous glass membrane. The surface of the Au electrodes prior to the NC adsorption was polished by diamond paste followed by a treatment in boiling concentrated HNO_3 and H_2SO_4. Then, the Au electrodes were thoroughly washed with doubly distilled water and annealed at 700 °C for 15 min in air. All measurements were performed in acetate buffer solution (0.1 M CH_3COONa + 0.0046 M CH_3COOH (pH 6)). Before the measurements, the Au electrodes were cycled in this electrolyte in the potential region from −0.5 to 1.2 V. The surface area of the Au electrodes was 2 cm^{-2}. The values of the current density were calculated by using the geometrical surface area of the electrodes.

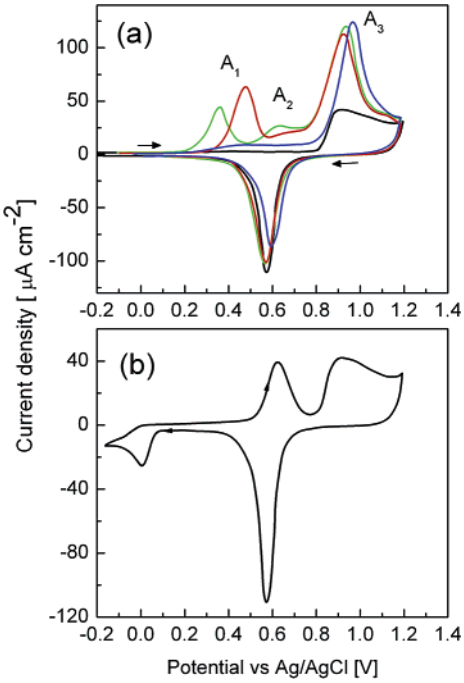

Figure 2. (a) Voltammograms of the bare Au electrode (black line) and the Au electrodes with preadsorbed ZnSe nanocrystals from two different fractions exhibiting excitonic maxima in the optical spectra at 3.65 (green) and 3.54 eV (red) and TGA molecules only (blue line). Electrolyte: acetic buffer solution (pH 6). (b) Cyclic voltammograms of the Au electrode in acetic buffer solution containing 0.001 M SeO_2 (pH 6). The potential sweep rate was 20 mV s^{-1}.

Typical cyclic voltammograms of a bare Au electrode and Au electrodes with two different fractions of ZnSe NCs preadsorbed are shown in Figure 2. The electrochemical oxidation of the bare gold electrode starts from 0.8 V with an anodic current peak at 0.91 V. In the reverse potential scan the cathodic current peak occurs at 0.57 V (Figure 2a, black line). In comparison with the bare electrode, the electrodes with adsorbed NCs exhibit three additional anodic peaks in the potential regions of 0.35−0.48 V (peak A_1), 0.63V (small peak A_2), and 0.89−0.93 V (peak A_3), respectively. The peaks A_1−A_3 are observed only in the first potential scan; in the second and subsequent scans these peaks are absent and the voltammogram is close to that for the bare gold electrode. The positions of the peaks A_1−A_3 are shifted into the positive direction by increasing the scan rate, which is indicative for an irreversibility of the processes responsible for these peaks. Since the thioglycolic acid molecules used as the stabilizers for the ZnSe NCs may themselves participate in the electrochemical reactions, we also recorded the voltammograms of the Au electrode with preadsorbed TGA molecules only. Electrooxidation of TGA adsorbed on the gold surface gives a small wave at 0.3−0.7 V and an anodic peak at 0.94 V (Figure 2a, blue line).

The evolution of the cyclic voltammograms of the ZnSe NCs during their photochemical treatment in the solution containing TGA and zinc ions is shown in Figure 3a. During the illumination the first anodic peak (A_1) is drastically shifted to more positive potentials and its charge increases while the position of the third peak (**A_3**) appears to be stable. It is noted that the position of the small second peak (A_2) becomes unrecognizable due to the masking of the moving first anodic

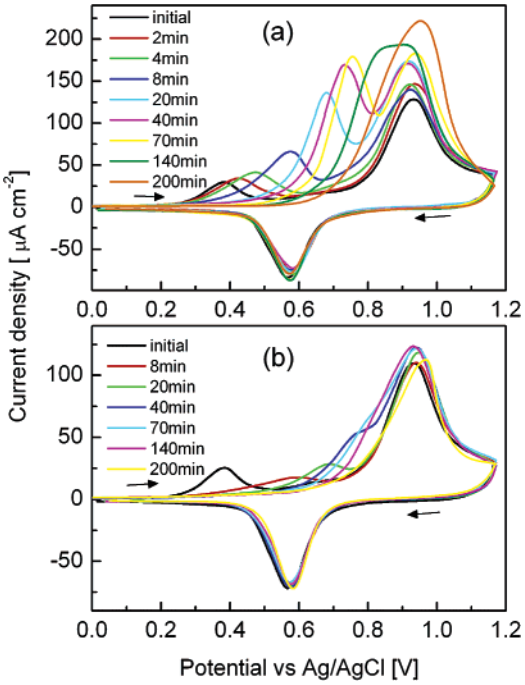

Figure 3. Evolution of the voltammograms of ZnSe NCs (position of the first excitonic maximum of the initial NC solution at 3.79 eV), preadsorbed on the Au electrodes, upon the time of the photochemical treatment of the ZnSe NCs colloids in solutions containing 16 mM $Zn(ClO_4)_2$ and 40 mM TGA (a) or 40 mM TGA only (b). The potential sweep rate was 20 mV s^{-1}.

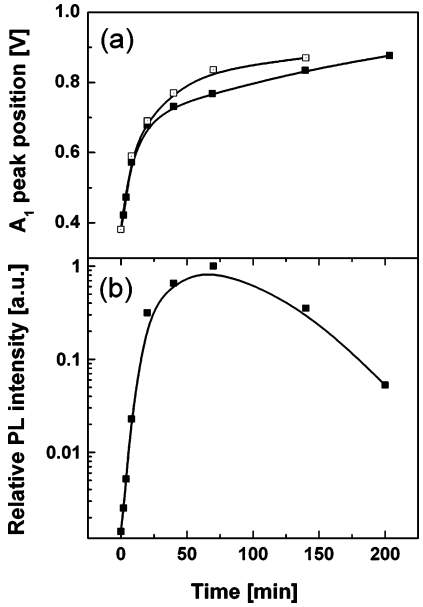

Figure 4. Evolution of the position of peak A_1 (a) and the relative PL intensity (b) of the ZnSe NCs during the NC photochemical treatment in solution containing 16 mM $Zn(ClO_4)_2$ and 40 mM TGA (full squares) and in solution containing 40 mM TGA only (open squares). After the phototreatment the ZnSe NCs were precipitated by 2-propanol and redissolved in acetate buffer for PL and electrochemical measurements.

peak (A_1). In Figure 4 the energetic position of peak A_1 and the PL intensity are presented as a function of the illumination time. The figure demonstrates a strong positive shift of the A_1 peak potential by more than 200 mV during the first 10−15 min of illumination, which is followed by a more smooth (quasilinear) evolution in the same potential direction with further increasing of the illumination time. The PL intensity increases during the first 70 min of illumination and then starts to decrease due to the photodegradation of the colloidal solution of ZnSe NCs.

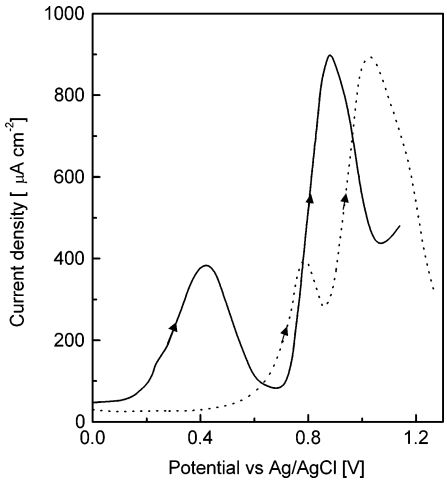

Figure 5. Anodic voltammograms of ZnSe (solid line) and ZnS (dotted line) thin film electrodes in a blank acetic buffer solution. The potential sweep rate was 20 mV s^{-1}.

The irradiation of the solution of the ZnSe NCs in the mixture with TGA only (i.e., without additional Zn^{2+} ions) demonstrates neither a PL intensity increase nor a shift in the absorption spectra while the CV curves show the typical strong shift of the first anodic peak (A_1) toward the positive direction (Figure 3b and Figure 4, open squares). It is obvious that the charge corresponding to peak A_1 is not notably altered in this case.

To gain a better understanding of the results obtained, the electrochemical behavior of polycrystalline ZnSe and ZnS thin films were studied additionally. The ZnSe films were deposited on Au plates under potentiostatic polarization ($E = -0.95$ V) in a solution containing 0.5 M $ZnSO_4$ + 0.001 M SeO_2, pH 2.5 ($T = 60$ °C) according to the method described previously.[19−21] The ZnS films were obtained on gold plates, using a pulsed deposition from a solution containing 30 mM $ZnSO_4$ + 5 mM $Na_2S_2O_3$ (pH 3) according to the procedure proposed by Fathy et al.[22] Just after the electrodeposition, the ZnSe and ZnS film electrodes were thoroughly rinsed with distilled water and immersed into the cell with acetate buffer solution (pH 6). Anodic oxidation of both ZnSe and ZnS films leads to the appearance of two anodic peaks on the voltammograms (Figure 5). The first peak is observed at about 0.4 V for ZnSe and at approximately 0.8 V for ZnS while the second peak appears at 0.88 and 1.03 V for ZnSe and ZnS, respectively.

According to the available literature data,[23−25] in the case of ZnSe the first peak can be assigned to the reaction

$$ZnSe \rightarrow Zn^{2+} + Se^0 + 2e^- \quad (1)$$

At potentials more positive than 0.7 V the complete oxidation of ZnSe becomes possible according to the reaction[25]

$$ZnSe \rightarrow Zn(II) + Se(IV) + 6e^- \quad (2)$$

Probably, similar processes occur during the electrochemical oxidation of the ZnS film electrodes.

Note that in going from ZnSe to ZnS, the potential of the first oxidation peak is shifted significantly into the positive direction (cf. Figure 5). The same is observed for peak A_1 when ZnSe NCs are treated photochemically for an extended period of time.

In analogy with our previous findings on similarly prepared CdTe NCs,[16] the first anodic peak (A_1) can be assigned to the

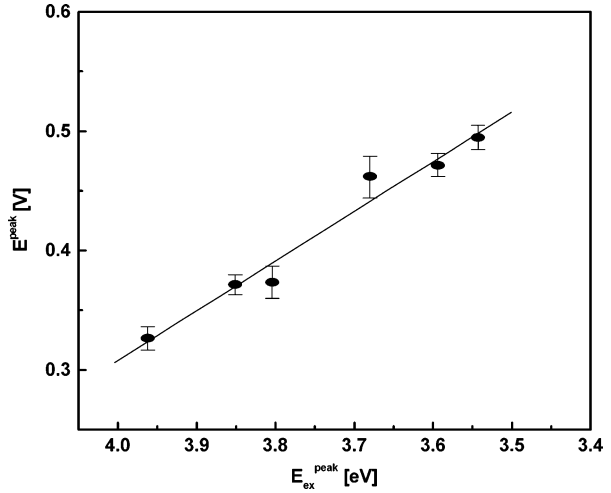

Figure 6. Dependence of the potential of peak A_1 derived from the CVs on the photon energy corresponding to first optical transition observed with the series of TGA-capped ZnSe NC size-selected fractions.

oxidation of the Se-related intra-band-gap surface states. The higher the quality was of the then investigated CdTe particles (higher PL quantum yield and enhanced stability) the less pronounced was peak A_1. Moreover, in the case of the CdTe NCs the position of this peak showed a size dependence, i.e., it was moving to lower energies (higher electrochemical potentials) with an increase of the NCs' size.[16] In the size range of 2 to ca. 4 nm this shift of A_1 amounts to a maximum of 120 mV.

For the ZnSe NCs studied here, the size range is not quite as large as that for the CdTe NCs. However, the ZnSe NCs exhibit first optical transitions between 312 and 350 nm and the maximum size dependent shift of the peak position of A_1 is about 170 mV. Also here peak A_1 moves to lower energies with increasing the NC size. Its potential depends linearly on the optical band gap of the nanoparticles (Figure 6) which is in accord with the findings for CdTe NCs.

During the photochemical treatment the shift of the first optical transition (from 336 to 365 nm equaling ca. 340 meV) is accompanied by a shift of the first anodic peak of as much as 400 mV. This behavior cannot be explained by the size dependence of the position of the anodic peak only. The change of the surface composition due to the formation of a thin shell around the ZnSe cores should also be taken into consideration. As seen from Figure 4a, a strong shift of the peak position is observed during the first 10−15 min of the photochemical treatment, indicating that the Se-related trap states disappear and S-related trap states become predominant on the NC surface. The energetic position of S-related surface states is assumed to be lower than that of the Se-related ones because the valence band of ZnS formed by S atoms is located significantly lower in energy than the ZnSe valence band formed by Se atoms.[26] The photochemically induced growing of the protecting ZnS shell improves the PL quantum yields of ZnSe NCs and is accompanied by a slower moving of the energy position of S-related surface states toward the valence band probably due to the increasing NC sizes. The increase in the total charge associated with peak A_1 is most likely the result of the growth of the ZnS shell during the photochemical treatment.

In the case of the illumination of the solution of ZnSe NCs in a mixture with TGA only the absence of Zn^{2+} ions in the solution makes impossible the photoassisted formation of the ZnS shell, which is necessary for the PL improvement.[4] At the same time photoexcitation of the ZnSe NCs may lead to dissolution of relatively unstable surface selenium atoms and/or to their replacement by sulfur appearing as a result of the TGA degradation. The replacement of the Se atoms by S atoms should result in an anodic shift of the oxidation peak A_1, which is nicely reflected in the experimental findings (Figures 3b and 4, open squares). However, the charge associated with peak A_1 is not noticeably changed in this case indicating that the ZnS shell does not grow, which is also an expected result keeping in mind that no additional Zn^{2+} ions are present in these sols.

When the phototreatment was performed in the absence of both Zn^{2+} ions and TGA in solution a complete degradation of the colloidal solution was observed in only a few minutes. In this period of time, the PL properties are not improved and a rapid decrease and disappearance of, first, the A_1 peak and subsequently the A_2 and A_3 peaks is observed in the voltammograms. This supports our assumption that TGA plays the role of acting both as a sulfur source and as a stabilizing agent for the NCs under phototreatment.

The third anodic peak (A_3) observed at the voltammograms can be assigned to the direct oxidation of the ZnSe NC cores according to reaction 2. In addition, TGA molecules also can be oxidized in the region of peak A_3 (Figure 2a). It should be noted that the potential corresponding to the peak of total electrochemical oxidation of semiconductor NCs in aqueous solutions may not correlate exactly with the valence band energy of these NCs due to a more complicated mechanism of their oxidation. A similar behavior was also observed for the TGA-capped CdTe NCs[16] as well as for thioglycerol-capped CdS NCs[10] and was attributed in both studies to a multielectron-transfer process where the charge carriers are consumed by fast coupled chemical reactions.

As for the second anodic peak (A_2), the origin is yet to be explained. In principle, it may be related to the anodic stripping of elemental Se forming as a result of electrooxidation of the Se-related surface states according to reaction 1.

The data on the electrochemical dissolution of small amounts of selenium, electrodeposited on a gold surface from a 10^{-3} M SeO_2 solution in acetic buffer (pH 6), may count in favor of this assumption. The corresponding voltammogram is shown in Figure 2b. The electrodeposition of Se on Au starts from 0.08 V with a cathodic peak at 0 V. During the reverse potential scan an anodic current peak corresponding to the Se dissolution is observed at 0.62−0.64 V, which is at a potential similar to that of peak A_2.

In summary, the evolution of the specific features in the cyclic voltammetric curves of ZnSe NCs as a function of their photochemical treatment is studied. The interpretation of the results based on the approaches developed for CdTe NCs is found to be in good correlation with the previously proposed mechanism of the ZnSe NCs phototreatment, i.e., the formation of a sulfur-enriched surface shell. By this, cyclic voltammetry has been demonstrated to be a powerful method for probing surface states of semiconductor NCs as well as for monitoring the evolution of these states during photochemical processing.

Acknowledgment. This work was supported by the EU Network of Excellence "PHOREMOST" and the EU project "STABILIGHT".

References and Notes

(1) Gaponik, N.; Talapin, D. V.; Rogach, A. L.; Hoppe, K.; Shevchenko, E. V.; Kornowski, A.; Eychmüller, A.; Weller, H. *J. Phys. Chem. B* **2002**, *106*, 7177.

(2) Jones, M.; Nedeljkovic, J.; Ellingson, R. J.; Nozik, A. J.; Rumbles, G. *J. Phys. Chem. B* **2003**, *107*, 11346.

(3) Bao, H.; Gong, Y.; Li, Z.; Gao, M. *Chem. Mater.* **2004**, *16*, 3853.
(4) Shavel, A.; Gaponik, N.; Eychmüller, A. *J. Phys. Chem. B* **2004**, *108*, 5905.
(5) Talapin, D. V.; Gaponik, N.; Borchert, H.; Rogach, A. L.; Haase, M.; Weller, H. *J. Phys. Chem. B* **2002**, *106*, 12659.
(6) van Dijken, A.; Janssen, A. H.; Smitsmans, M. H. P.; Vanmaekelbergh, D.; Meijerink, A. *Chem. Mater.* **1998**, *10*, 3513.
(7) Wang, Y.; Tang, Z.; Correa-Duarte, M. A.; Liz-Marzan, L. M.; Kotov, N. A. *J. Am. Chem. Soc.* **2003**, *125*, 2830.
(8) Wang, Y.; Tang, Z.; Correa-Duarte, M. A.; Pastoriza-Santos, I.; Giersig, M.; Kotov, N. A.; Liz-Marzan, L. M. *J. Phys. Chem. B* **2004**, *108*, 15461.
(9) Murase, N.; Gao, M. Y.; Gaponik, N.; Yazawa, T.; Feldmann, J. *Int. J. Mod. Phys. B* **2001**, *15*, 3881.
(10) Haram, S. K.; Quinn, B. M.; Bard, A. J. *J. Am. Chem. Soc.* **2001**, *123*, 8860.
(11) Kucur, E.; Riegler, J.; Urban, G. A.; Nann, T. *J. Chem. Phys.* **2003**, *119*, 2333.
(12) Ogawa, S.; Hu, K.; Fan, F.-R. F.; Bard, A. J. *J. Phys. Chem. B* **1997**, *101*, 5707.
(13) Chen, S. W.; Truax, L. A.; Sommers, J. M. *Chem. Mater.* **2000**, *12*, 3864.
(14) Bae, Y.; Myung, N.; Bard, A. J. *Nano Lett.* **2004**, *4*, 1153.
(15) Kucur, E.; Bucking, W.; Giernoth, R.; Nann, T. *J. Phys. Chem. B* **2005**, *109*, 20355.
(16) Poznyak, S. K.; Osipovich, N. P.; Shavel, A.; Talapin, D. V.; Gao, M.; Eychmüller, A.; Gaponik, N. *J. Phys. Chem. B* **2005**, *109*, 1094.
(17) In a typical synthesis 0.875 g (2.35 mmol) of $Zn(ClO4)_2 \cdot 6H_2O$ was dissolved in 125 mL of water, and 5.7 mmol of thioglycolic acid was added under stirring, followed by adjusting of the pH by dropwise addition of a 1 M solution of NaOH to 6.5. The solution was placed in a three-necked flask fitted with a septum and valves and was deaerated by N_2 bubbling for 1 h. Under stirring, H_2Se gas (generated by the reaction of 0.134 g (0.46 mmol) of Al_2Se_3 lumps with an excess amount of 1 N H_2SO_4 under N_2 atmosphere) was passed through the solution together with a slow nitrogen flow for nearly 20 min. ZnSe precursors were formed at this stage. The further nucleation and growth of the nanocrystals proceeded upon refluxing at 100 °C under open-air conditions with a condenser attached.
(18) Talapin, D. V.; Rogach, A. L.; Shevchenko, E. V.; Kornowski, A.; Haase, M.; Weller, H. *J. Am. Chem. Soc.* **2002**, *124*, 5782.
(19) Riveros, G.; Gomez, H.; Henriquez, R.; Schrebler, R.; Cordova, R.; Marotti, R. E.; Dalchiele, E. A. *Bol. Soc. Chil. Quim.* **2002**, *47*, 411.
(20) Riveros, G.; Gomez, H.; Henriquez, R.; Schrebler, R.; Marotti, R. E.; Dalchiele, E. A. *Sol. Energy Mater. Sol. Cells* **2001**, *70*, 255.
(21) Bouroushian, M.; Kosanovic, T.; Loizos, Z.; Spyrellis, N. *J. Solid State Electrochem.* **2002**, *6*, 272.
(22) Fathy, N.; Kobayashi, R.; Ichimura, M. *Mater. Sci. Eng. B* **2004**, *B107*, 271.
(23) de Wit, A. R.; Kelly, J. J. *J. Electroanal. Chem.* **1994**, *366*, 163.
(24) Gautron, J.; Lemasson, P.; Rabago, F.; Triboulet, R. *J. Electrochem. Soc.* **1979**, *126*, 1868.
(25) Lemasson, P.; Gautron, J. *J. Electroanal. Chem.* **1981**, *119*, 289.
(26) Faschinger, W. *J. Cryst. Growth* **1999**, *197*, 557.